



## OPEN Combination of paclitaxel with rosiglitazone induces synergistic cytotoxic effects in ovarian cancer cells

Binita Patel<sup>1</sup>, Shanaya Patel<sup>2</sup>, Foram Modi<sup>3</sup>, Aditi Patel<sup>2</sup>, Brijesh Gelat<sup>3</sup>, Vivek Tanavde<sup>2</sup>, Abhay Vasavada<sup>4</sup> & Kaid Johar SR<sup>3</sup>✉

Ovarian cancer is known to be a challenging disease to detect at an early stage and is a major cause of death among women. The current treatment for ovarian cancer typically involves a combination of surgery and the use of drugs such as platinum-based cytotoxic agents, anti-angiogenic drugs, etc. However, current treatment methods are not always effective in preventing the recurrence of ovarian cancer. As a result, the treatments administered after a relapse need to be more aggressive, leading to increased toxicity and drug resistance. To address this issue, researchers are exploring the potential of combining existing anticancer agents with novel or repurposed drugs to reduce the side effects and improve the effectiveness of treatment. In this study, we have investigated the use of rosiglitazone, a well-known anti-diabetic drug, in combination with the chemotherapeutic drug, paclitaxel for the prevention of ovarian cancer. The study utilized the SKOV-3 ovarian cancer cell line to assess the effects of this combination treatment. The results of the study showed that the combination of paclitaxel with rosiglitazone inhibited cell proliferation at much lower concentrations of paclitaxel as compared to paclitaxel alone. The combined treatment also induced cell cycle arrest at the G2/M phase and increased apoptosis by altering the mitochondrial membrane potential of the cells. Additionally, the combination treatment activated the PPAR- $\gamma$  pathway and downregulated expression of genes associated with cancer stemness, such as NANOG, OCT4, and EHF. Furthermore, the CAM assay substantiated the anti-angiogenic potential of the synergistic treatment of paclitaxel and rosiglitazone. The findings of the study suggest that repurposing rosiglitazone as an anticancer agent in combination with paclitaxel has immense potential to target cancer cell cycle progression and apoptosis, making it a promising therapeutic approach for sensitizing chemo-resistant population of ovarian cancer cells.

**Keywords** Ovarian cancer, Paclitaxel, Rosiglitazone, SKOV-3, Synergism, Anticancer

In 2022, global data from Globocan indicates that the number of cancer cases rose to 20 million, resulting in 9.7 million cancer-related fatalities<sup>1</sup>. The World Health Organization in 2022 reported that there are 324,398 new cases of ovarian cancer, with 206,839 resulting in death. In India, ovarian cancer ranks as the third most prevalent cancer among females, with 47,333 new cases diagnosed, accounting for 6.6% of all cancers diagnosed in women. Ovarian cancer, a diverse disease with a 5-year relative survival rate and bleakest prognosis, is a prevalent form of gynecological cancer<sup>2</sup>. Epithelial ovarian cancer (EOC) is the primary reason behind the most deaths among all gynecological cancers, accounting for 90% of ovarian malignancies. EOC is typically diagnosed at advanced stages III or IV, leading to a grim prognosis<sup>3,4</sup>. In India, ovarian cancer is estimated to have the second-highest incidence rate globally<sup>5</sup>.

Surgery and chemotherapy are the main treatments for ovarian cancer; However, patients often experience a recurrence with resistance to chemotherapy within a few years of the initial treatment<sup>6</sup>. Initially, for ovarian cancer melphalan was commonly used as a single-agent chemotherapy, but it has been since supplanted by a

<sup>1</sup>Department of Life Sciences, School of Sciences, Gujarat University, Ahmedabad 380009, Gujarat, India. <sup>2</sup>Division of Biological and Life Sciences, School of Arts and Sciences, Ahmedabad University, Central Campus, Ahmedabad 380009, Gujarat, India. <sup>3</sup>Department of Zoology, Biomedical Technology, Human Genetics, and WBC, School of Sciences, Gujarat University, Ahmedabad 380009, Gujarat, India. <sup>4</sup>Iladevi Cataract and IOL Research Centre, Memnagar, Ahmedabad 380052, Gujarat, India. ✉email: kaidjohar@gujuni.ac.in

combination therapy involving doxorubicin and cisplatin. By the early 1990s, paclitaxel (PTX) emerged as a highly effective treatment option for platinum-resistant ovarian cancer<sup>7</sup>. PTX has a similar type of side effects as that of other therapeutic agents' carboplatin, and doxorubicin and these effects are dependent on the number of chemotherapeutic drugs used for the treatment<sup>8</sup>. Therefore, it is desirable to reduce the amount of PTX for the treatment while maintaining its effectiveness of the treatment. Hence, synergistic treatment of PTX with another molecule that can target similar or other mechanisms involved in the development of ovarian cancer is required<sup>9</sup>. Incorporating a biological agent alongside a PTX presents a promising option to maximize therapeutic benefits while minimizing toxicity<sup>10</sup>.

The process of discovering a new therapeutic agent is complex, time-consuming, and costly<sup>11</sup>. In such scenarios, drug repurposing offers numerous advantages compared to the challenges associated with finding new agents<sup>12</sup>. Nuclear receptor-targeting drugs are used for the treatment of various diseases. About 13% of the drugs currently on the market target nuclear receptors<sup>13</sup>. PPAR- $\gamma$  is a highly conserved nuclear receptor expressed throughout the body<sup>14,15</sup> and shown to play a critical role in cell differentiation, apoptosis, angiogenesis, and epithelial-mesenchymal transition. PPAR- $\gamma$  has been shown to inhibit inflammation and cell migration by targeting the PTEN pathway<sup>16,17</sup>. Several studies have found that PPAR- $\gamma$  is dysregulated in various cancers<sup>18–20</sup>. PPAR- $\gamma$  is shown to activate the intrinsic apoptotic pathway in breast cancer cells and enhance the sensitivity of pancreatic cancer cells to radiotherapy<sup>21,22</sup>. Hence, exciting the PPAR- $\gamma$  can be an option for the treatment of ovarian cancer.

The synthetic ligands for PPAR- $\gamma$ , such as thiazolidinediones (TZDs) like rosiglitazone, troglitazone, pioglitazone, and ciglitazone have been developed primarily for treating type II diabetes. Though these TZDs including rosiglitazone are associated with side effects, they are still used as add-ons to more popular therapies of type II diabetes. These TZDs are also evaluated as therapeutic agents for the treatment of other diseases, including cancers<sup>23,24</sup>. Rosiglitazone (RGZ), one such TZD, has been shown to induce apoptosis and autophagy, inhibit cell proliferation and metastasis, reverse multidrug resistance, reduce immune suppression, and inhibit angiogenesis through the PPAR- $\gamma$  dependent pathway in ovarian cancer cell line<sup>25,26</sup>. RGZ down-regulates FZD1 and MDR1/P-gp expression in a concentration-dependent manner and suppresses the development of drug resistance cancer through the Wnt/ $\beta$ -catenin pathway<sup>27</sup>. Therefore, RGZ can be a potential PPAR- $\gamma$  agonist along with paclitaxel (PTX) for the treatment of ovarian cancer.

In the present study, we have evaluated RGZ along with PTX as a synergistic therapy for the treatment of epithelial ovarian cancer on the SKOV-3 cell line. The safety and effectiveness of each drug alone and in combination were assessed using the MTT assay. Additionally, the effects of the combination therapy on nuclear fragmentation, cell cycle progression, cell death, mitochondrial function, expression of cancer stem cell genes, and angiogenesis were evaluated.

## Results

### Synergistic treatment induced cytotoxic effect

The cytotoxic impact of rosiglitazone (RGZ), paclitaxel (PTX), and a combination of them was assessed using the MTT assay after 24 h of treatment. The results revealed that PTX, RGZ, and their combination was effective in reducing cell survival in a dose-dependent manner. PTX displayed an IC<sub>50</sub> value of 25 nM, whereas RGZ exhibited an IC<sub>50</sub> value of 25  $\mu$ M (Fig. 1). Interestingly, the combination treatment had an IC<sub>50</sub> of 1 nM for PTX and 0.5  $\mu$ M for RGZ (Fig. 1) which is significantly less than that of RGZ and PTX alone. These findings suggest that the synergistic effect of PTX and RGZ can effectively hinder cell proliferation at much lower concentrations than those required for individual treatments. Based on these findings, concentrations of 1 nM for PTX and 0.5  $\mu$ M for RGZ were selected for further analysis.

Combination index analysis (Fig. 2) showed that CI value of RGZ with PTX is less than 1 which indicates that this combination is highly synergistic to each other. Table 1 shows different CI values at different concentrations of RGZ and PTX.

### Synergistic treatment-induced G2/M arrest

We have analyzed the effect of the combinatorial treatment of PTX and RGZ on the distribution of SKOV-3 cells in the different phases of cell cycle. Most of the cells treated with PTX + RGZ were found in the G2/M phase ( $P < 0.001$ ) along with a reduction in the number of cells in the G0/G1 ( $P < 0.001$ ) and S phase ( $P < 0.001$ ) compared to that of control (Fig. 3). There was a notable increase in the accumulation of cells in the sub-G0/G1 phase in the RGZ alone treated group compared to the control, PTX alone, and PTX + RGZ group. The substantial increase in the number of cells in G2/M phase suggests that the cells were arrested in this stage of cell cycle due to the treatment of PTX compared to control and RGZ alone. In the combination treatment group, the number of accumulated cells in the sub-G0/G1 phase is lesser than in the RGZ-treated group while the number of cells in the G2/M phase is more in PTX alone compared to PTX + RGZ and control.

### Synergistic treatment induces apoptosis

One of the best hallmarks of apoptosis is the condensation followed by fragmentation of the nuclei. We have labeled nuclei with propidium iodide (PI) observed under the fluorescence microscope and images were captured. The number of condensed nuclei was counted. Following treatment with PTX + RGZ, there was a notable increase in the number of condensed nuclei compared to that of control ( $P < 0.001$ ), PTX alone ( $P < 0.001$ ), and RGZ alone ( $P < 0.001$ ) (Fig. 4).

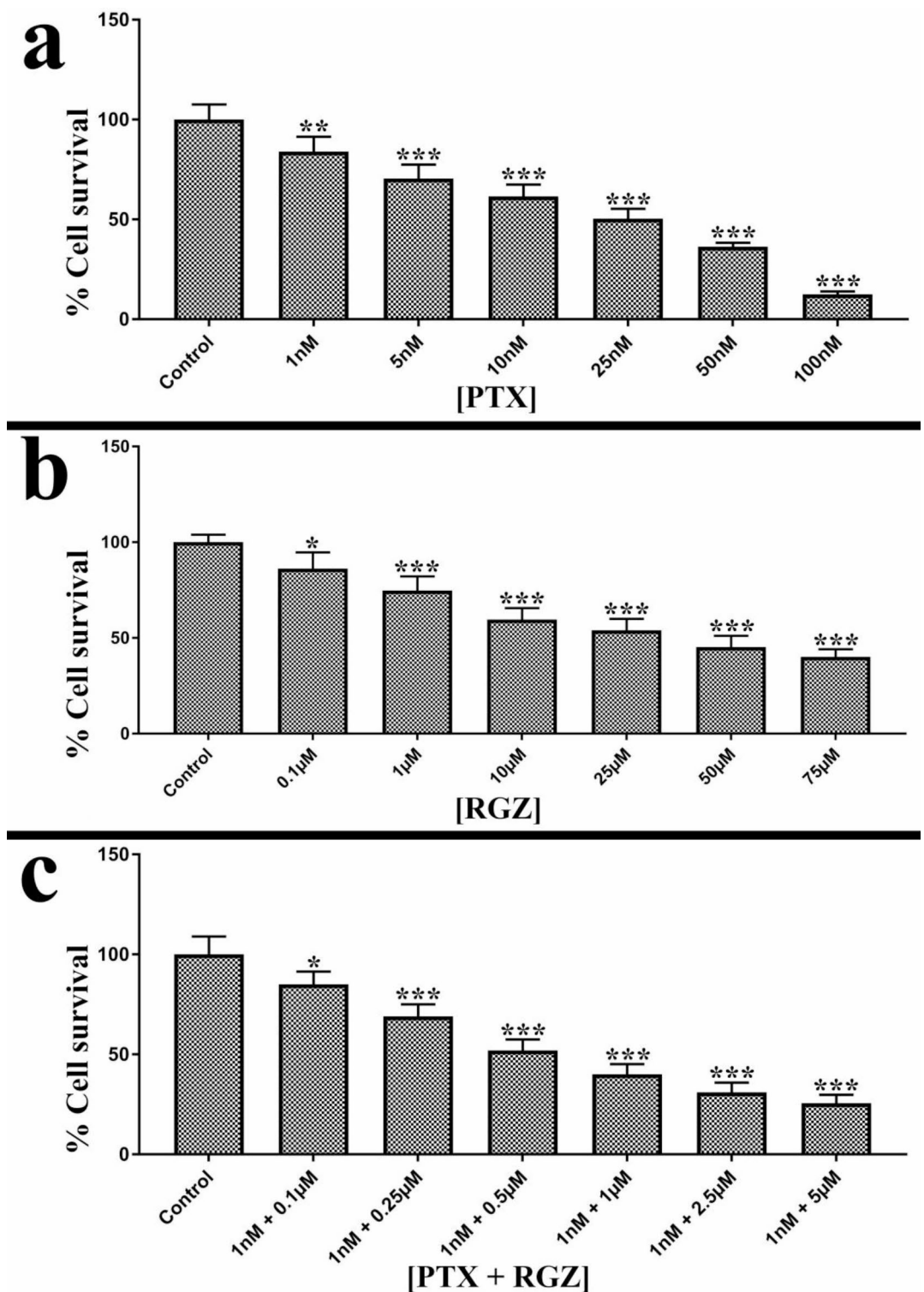


**Fig. 1.** Cytotoxic effect of paclitaxel (PTX) and rosiglitazone (RGZ) on SKOV-3 ovarian cancer cells. (a) Percentage cell survival after 24 h treatment of 1 nM, 5 nM, 10 nM, 25 nM, 50 nM and 100 nM PTX. (b) Percentage cell survival after 24 h of treatment of 0.1 μM, 1 μM, 10 μM, 25 μM, 50 μM, 75 μM RGZ. (c) Percentage cell survival after 24 h of combined treatment of 0.1 μM, 0.25 μM, 0.5 μM, 1 μM, 2.5 μM and 5 μM of RGZ and 1 nM PTX. Error bars represent the mean  $\pm$  SEM of three independent experiments. \* $p < 0.05$ , \*\* $p < 0.01$  and \*\*\* $p < 0.001$  as compared to that of the control.

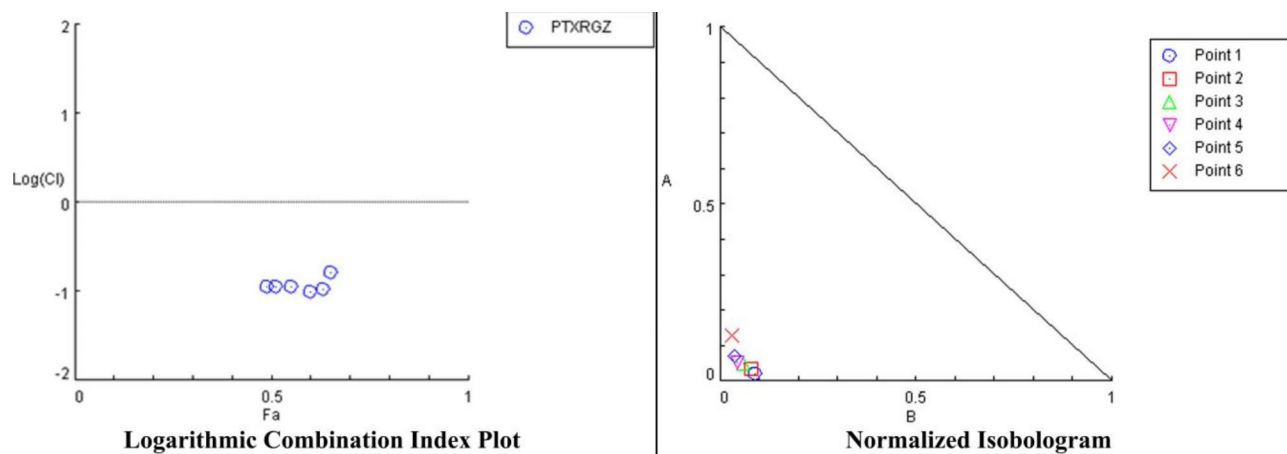


**Fig. 2.** Logarithmic combination index plot and normalized isobologram for rosiglitazone (RGZ) and paclitaxel (PTX).

Rosiglitazone (nM)	Paclitaxel (nM)	CI values
500	1	0.11194
1000	1	0.11320
2500	1	0.11207
5000	1	0.09698
10,000	1	0.10606
25,000	1	0.16282

**Table 1.** Combination index (CI) value of paclitaxel (PTX) and rosiglitazone (RGZ).

### Synergistic treatment reduces mitochondrial membrane potential

JC-1 is a positively charged fluorescent dye that is utilized to pinpoint the physiological state of mitochondria within the cells. In healthy cells, JC-1 forms J-aggregates that emit red fluorescence. Conversely, in unhealthy cells, J-aggregates fail to form, and JC-1 remains in its monomeric state, emitting green fluorescence. Our findings indicate that the ratio of red to green fluorescence cells decreases in cells treated with PTX and RGZ. Furthermore, there is a notable decrease in the red-to-green fluorescence ratio in cells treated with both RGZ and PTX in combination, as compared to cells treated with RGZ or PTX alone, as well as the control (Fig. 5).

### Synergistic treatment reduces the expression of cancer stemness markers and increases the expression of PPAR- $\gamma$

The impact of RGZ and PTX on cancer stemness genes and PPAR- $\gamma$  was carefully assessed. Our results demonstrate a notable decrease in the expression of EHF, OCT4, and NANOG due to combined treatment of PTX and RGZ. The gene expression levels of EHF, OCT4, and NANOG were reduced by 77% ( $P < 0.001$ ), 75% ( $P < 0.001$ ), and 80% ( $P < 0.001$ ) respectively in the PTX + RGZ treated samples compared to the control, PTX alone and RGZ alone (Fig. 6). Given that RGZ acts as a specific agonist for the PPAR- $\gamma$  receptor, it was crucial to examine the effect of combinatorial treatment on the protein expression levels of PPAR- $\gamma$ . Along with PPAR- $\gamma$ , we have also studied the protein expression of  $\beta$ -actin and PPAR- $\alpha$  to normalize the expression of PPAR- $\gamma$ . As compared to  $\beta$ -actin, there is little decrease in the expression of PPAR- $\gamma$  due to PTX treatment but increased 300 times after RGZ treatment ( $P < 0.001$ ) and 400 times after the combination treatment of PTX with RGZ ( $P < 0.001$ ) compared to that of control (Fig. 7). As compared to PPAR- $\alpha$  also, PPAR- $\gamma$  level increased 350 times after RGZ treatment ( $P < 0.001$ ) and 275 times after the combination treatment of PTX with RGZ ( $P < 0.001$ ) compared to that of control. Hence, the exposure of RGZ alone as well as RGZ with PTX increased the expression of PPAR- $\gamma$  (Fig. 6).

### Synergistic treatment inhibits angiogenesis in the CAM model

An angiogenesis assay was conducted to assess the effectiveness of combined treatment in the CAM (chick chorioallantois membrane) in-vivo model. We have measured the number of micro-vessels of the same region at 0 h and after 24 h of exposure to explain the effect of treatment on angiogenesis. Our result shows that treatment of PTX alone, RGZ alone, and a combination of PTX with RGZ decreased the number of micro-vessels. However, the effect was highest in the combination treatment of PTX with RGZ compared to that of control, PTX alone and RGZ alone (Fig. 8).

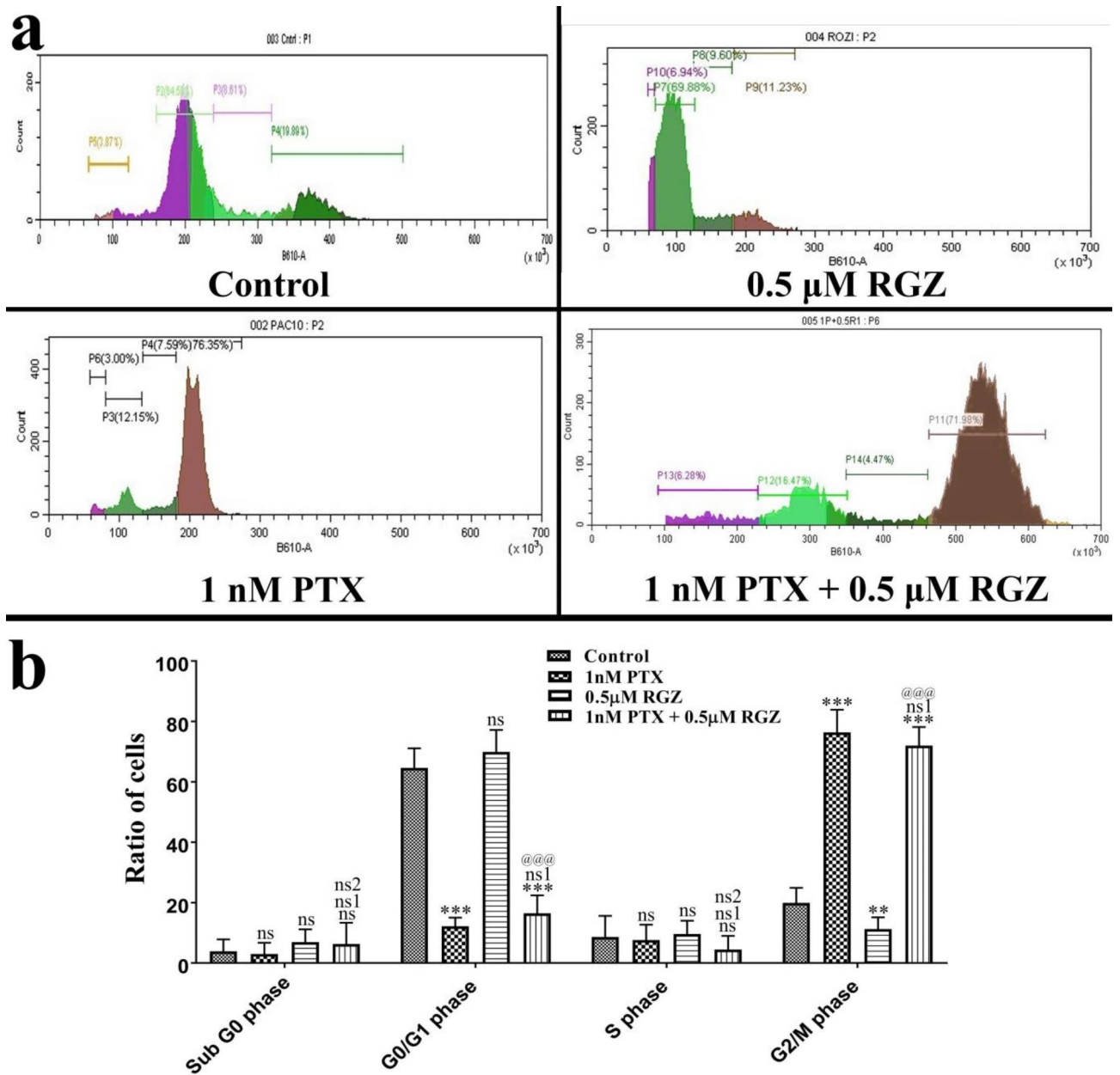


**Fig. 3.** Synergistic treatment of paclitaxel (PTX) and rosiglitazone (RGZ) on the cell cycle of SKOV-3 ovarian cancer cells. **(a)** Cell cycle distribution. **(b)** Percent alteration in the cell cycle in control and combination treatment of PTX and RGZ groups. Error bars represent the mean  $\pm$  SEM of three independent experiments. ns = non-significant, \*\* $p < 0.01$  and \*\*\* $p < 0.001$  as compared to that of the control. ns1 non-significant as compared to that of PTX alone. ns2 non-significant, @@@ $p < 0.001$  as compared to that of RGZ alone.

### Discussion

The use of synergistic therapy offers numerous benefits compared to monotherapy<sup>10</sup>. Synergism of two or more drugs can overcome toxicity and other side effects on tissues which are associated with high doses of each individual compound by either countering biological compensation or sparing doses on each compound. Moreover, synergism treatment can improve the efficiency of the treatment and reduce the development of drug resistance<sup>33</sup>. Research conducted by Miao and his colleagues corroborates our results, indicating that PPAR- $\gamma$  agonist along with all-trans retinoic acid not only regulates lipid and glucose metabolism but also plays a crucial role in promoting tumor cell differentiation, inducing apoptosis, and suppressing tumor angiogenesis in human colorectal cancer cell line<sup>34</sup>. Considering this, our research focuses on utilizing a combination of drugs to potentially target the aggressive ovarian cancer cells. Specifically, we have combined the traditional chemotherapeutic drug paclitaxel (PTX) with rosiglitazone (RGZ) to enhance treatment efficacy and minimize adverse effects. We have chosen the SKOV-3 ovarian cancer cell line for our current research, known for its resistance to tumor necrosis factor and various cytotoxic drugs like diphtheria toxin, cisplatin, and adriamycin<sup>52</sup>.

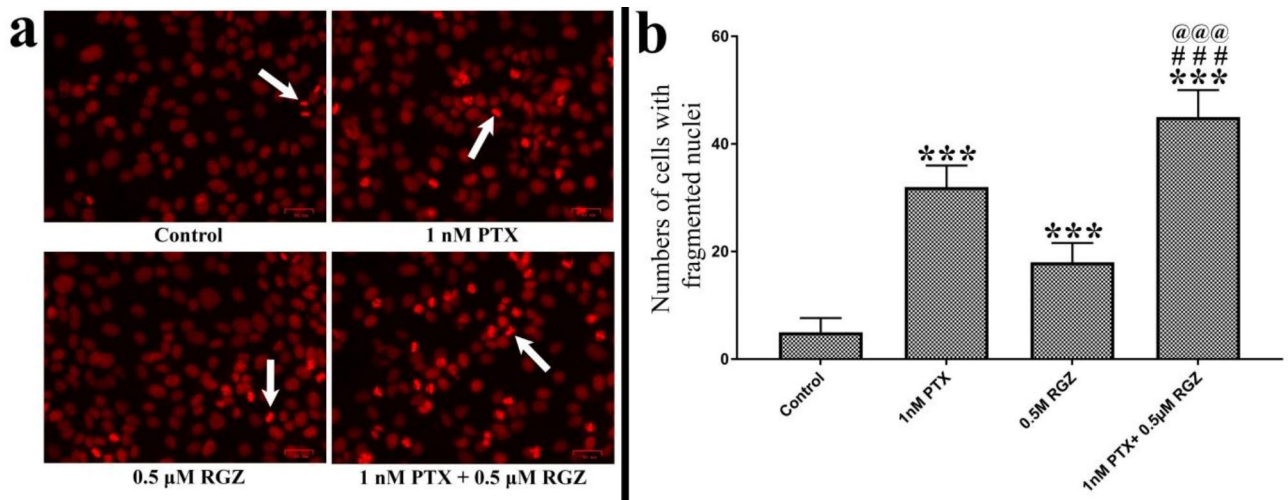


**Fig. 4.** Effect of paclitaxel (PTX) and rosiglitazone (RGZ) on the nuclear fragmentation of SKOV-3 ovarian cancer cells. **(a)** Nuclei stained with propidium iodide. Scale bar 34 μm. **(b)** Number of fragmented nuclei in control and combination treatment of PTX and RGZ (1 nM + 0.5 μM) groups. Error bars represent the mean ± SEM of three independent experiments. \*\*\* $p < 0.001$  as compared to that of the control. ### $p < 0.001$  as compared to that of the PTX alone. @@@ $p < 0.001$  as compared to that of the RGZ group.

We investigated the effects of a combination treatment on the SKOV-3 cell line both in vitro and using the CAM in vivo model. Our findings demonstrate that the synergistic treatment leads to a decrease in mitochondrial membrane potential, triggers apoptosis, halts cell cycle progression and decreases cancer stemness in the SKOV-3 cell line and impedes angiogenesis in the CAM model. Due to the inclusion of RGZ along with PTX in the current study, we were able to reduce the dose of PTX considerably to induce changes like or even better than that of PTX alone. Reduction in the amount of PTX can directly reduce the PTX-related side effects.

The current research utilized the MTT assay to assess cellular metabolic activity and cytotoxicity. The study found a notable reduction in the need for the chemotherapeutic agent, PTX. This suggests that using PTX together with RGZ could be an effective treatment for drug-resistant SKOV-3 ovarian cancer cells<sup>25,35</sup>. Sheu and her team previously discovered that RGZ can inhibit the proliferation of endothelial cells in the human umbilical vein by targeting key cell cycle regulators<sup>36</sup>. In this study, we evaluated dose-effect curve of RGZ and PTX to find out the synergism between these two drugs. Combination index values in the SKOV-3 cell line showed below 1 which indicate strong synergism of RGZ and PTX.

Our findings reveal that the combined treatment of PTX and RGZ leads to a significant increase in the number of cells arrested in the G2/M phase of the cell cycle. This combination treatment also results in an enhanced population of cells in the sub G0 phase and a decrease in the G0/G1 phase compared to the control group. Wang and his colleagues observed that the synergistic effects of vincristine and RGZ treatment unregulated cyclin B1 and down-regulate pcdc2 genes, which cause cell arrest in the G2/M phase of the cell cycle in oral epidermoid carcinoma cells<sup>37</sup>.

Our findings reveal that the ratio of red to green fluorescence was notably lower in cells treated with PTX + RGZ compared to those treated with only RGZ or PTX, suggesting a potential involvement of programmed cell death through the intrinsic apoptosis pathway. Previous research has demonstrated that combination therapy of rosiglitazone and ranpirnase can kick start significant depolarization of the mitochondrial membrane, trigger nuclear fragmentation, and initiate apoptosis<sup>38,39</sup>. Thus, through modifications in mitochondrial metabolism and membrane potential, cancer cells can become more susceptible to treatment methods that aim at disrupting other vital functions such as cell cycle progression and initiation of cell death<sup>40</sup>.

In addition, RGZ has been found to induce apoptosis by upregulating the expression of PTEN in hepatocellular carcinoma and facilitating apoptosis in ovarian cancer when combined with olaparib<sup>41,42</sup>. Treatment with RGZ has also been shown to down-regulate Bcl-2 and survivin, up-regulate the BAX gene, and activate caspase 3 to induce apoptosis in carcinoma cell lines<sup>43</sup>. Thus, these collective observations indicate that the synergistic treatment of PTX and RGZ enhances the anti-proliferative response, suppresses self-renewal, and induces apoptosis more effectively than individual treatment.

Moreover, we assess how combination therapy impacts the activity of cancer stemness genes. Various studies have shown that upregulation of EHF, OCT4, and NANOG promotes cell growth, migration, resistance to chemotherapy, advancement of cancer, tumor formation, development of cancer stem cells, and malignancy<sup>44–48</sup>. Noteworthy findings from our current research reveal reduced levels of cancer stemness genes NANOG, OCT4, and EHF in synergistic treatment. Significantly, there was a rise in the protein levels of PPAR-γ in combined treatment as opposed to individual treatments with RGZ and PTX. This suggests that an increase in PPAR-γ triggers a PPAR-γ-dependent pathway, ultimately leading to decreased expression of the three stemness marker genes. Inhibition of EHF has been shown to curb the invasion, growth, and tumor formation of ovarian cancer

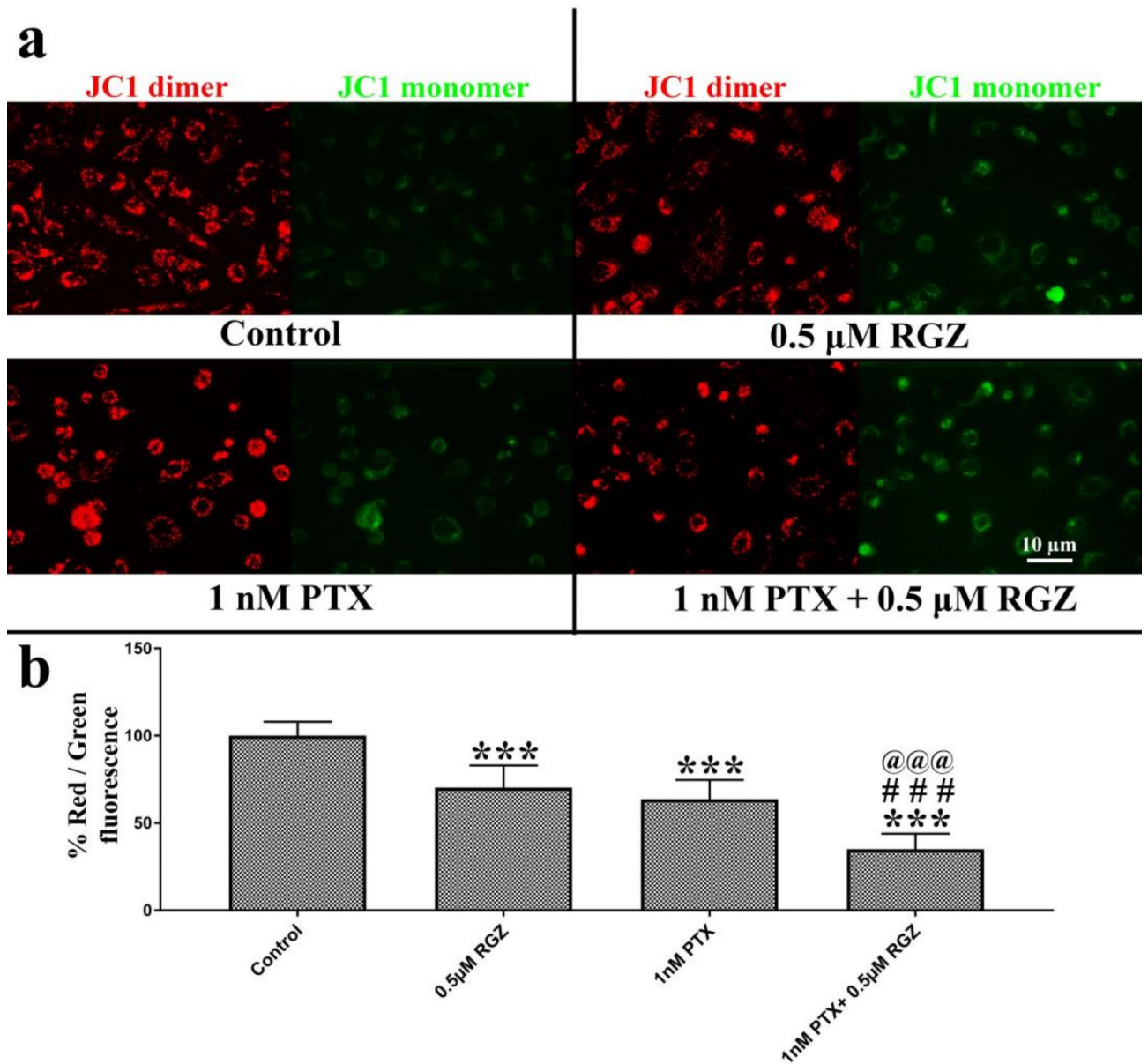


**Fig. 5.** Effect of paclitaxel (PTX) and rosiglitazone (RGZ) on the mitochondrial membrane potential in SKOV-3 ovarian cancer cells. **(a)** Mitochondria were stained by JC-1 fluorescent dye. Red-colored mitochondria have their membrane polarized while green stain represents unpolarized mitochondria. **(b)** Percent ratio of red versus green fluorescence in SKOV-3 ovarian cancer cells. Error bars represent the mean  $\pm$  SEM of three independent experiments. \*\*\* < 0.001 as compared to that of the control. ### < 0.001 as compared to that of the PTX alone. @@@ < 0.001 as compared to that of the RGZ alone.

cells<sup>49</sup>. Lowered expression of NANOG, OCT4, and EHF alongside increased expression of PPAR- $\gamma$  likely regulates the activity of crucial genes that contribute to the formation of the stem cell “Niche” in ovarian cancer.

Angiogenesis plays a crucial role in cancer growth as solid tumors need a blood supply to continue growing and spreading. Lokman and his team illustrated that the CAM assay is an effective and cost-efficient method for studying the spread of ovarian cancer cells<sup>31</sup>. Additionally, PPAR- $\gamma$  is highly present in the cells that line tumor blood vessels and can hinder tumor growth by stopping angiogenesis<sup>24,50</sup>. It has also been found that PTX can reduce the levels of vascular endothelial growth factor (VEGF) in tumors<sup>51</sup>. Previous research by Sheu and his team demonstrated that RGZ notably reduced VEGF-induced tube formation and movement of endothelial cells, likely due to disruptions in the actin cytoskeleton<sup>36</sup>. Building on previous studies, our research reveals a significant decrease in the number of small blood vessels in the group treated with PTX + RGZ compared to those treated with just RGZ, PTX, or control.

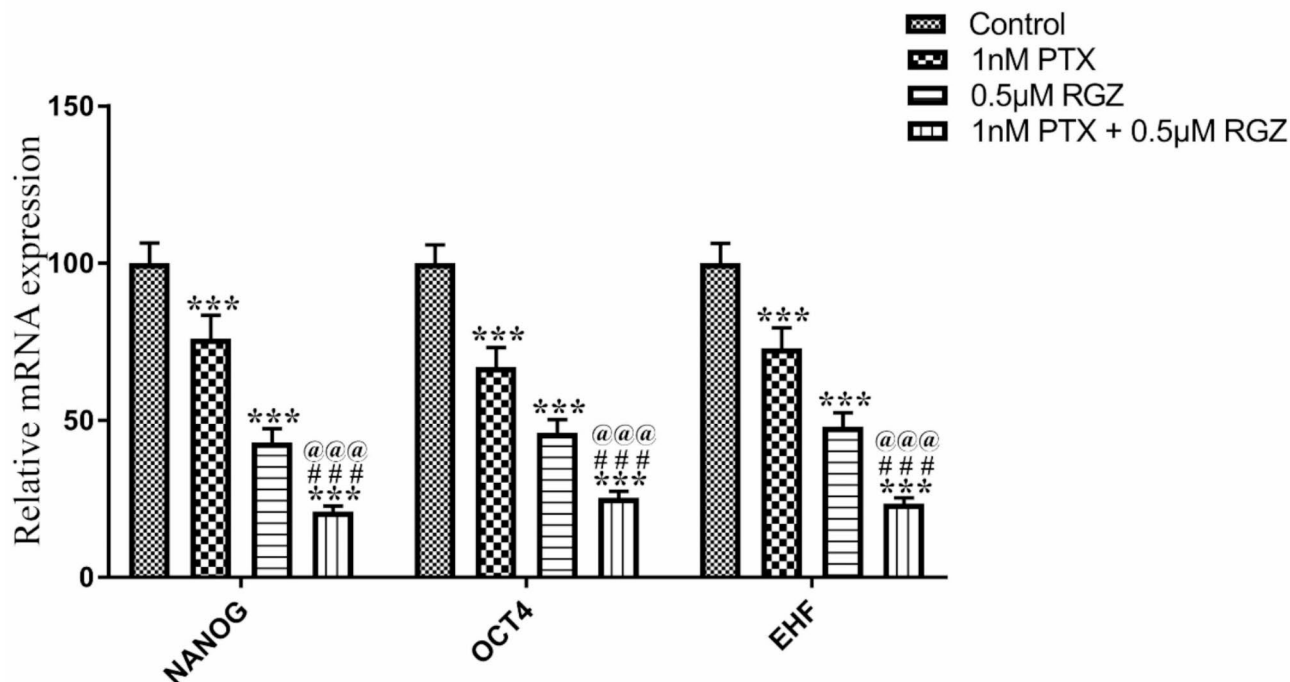


**Fig. 6.** Effect of paclitaxel (PTX) and rosiglitazone (RGZ) on the mRNA expression of stemness determining genes in SKOV-3 ovarian cancer cells. GAPDH was used as a housekeeping gene. Error bars represent the mean  $\pm$  SEM of three independent experiments. \*\*\* $<$ 0.001 as compared to that of the control. ### $<$ 0.001 as compared to that of the PTX alone. @@@ $<$ 0.001 as compared to that of the RGZ alone.

## Conclusion

The emergence of drug resistance in ovarian cancer significantly correlates with a decline in clinical outcomes and severely restricts the effectiveness of existing cancer therapies. Growing evidence indicates that increased expression of certain proteins and modifications to signaling pathways are responsible for chemo-resistant ovarian cancer.

Therefore, there is a need for emerging synergistic therapies that utilize chemotherapeutic agents at lower concentrations along with other drugs to overcome the resistant effect of conventional cancer drugs along with providing effects to other therapeutic targets. The findings of this study demonstrate that the combination of rosiglitazone with paclitaxel inhibits cell proliferation and promotes apoptosis in SKOV-3 ovarian cancer cells that are resistant to tumor necrosis factor along with inhibition of angiogenesis in CAM in vivo model. This synergistic effect of rosiglitazone with paclitaxel appears to be mediated by the activation of PPAR- $\gamma$  and the suppression of cancer stemness genes. Investigating this synergistic therapy in different ovarian cancer cell lines, primary cells, and patient-derived cells is crucial to determine its specificity and effectiveness.

## Methodology and materials

### Cell culture and maintenance

The SKOV-3 human ovarian adenocarcinoma cell line was procured from the National Centre for Cell Science (NCCS) in Pune, Maharashtra, India. The cells were grown in DMEM-F12 (Dulbecco's Modified Eagle Medium/Nutrient Mixture F-12, Hyclone) medium supplemented with 10% FBS (Fetal bovine serum, Hyclone) and penicillin, streptomycin, amphotericin B antibiotics at 37 °C with 5% CO<sub>2</sub>. Subculturing was done when cells reached 70% confluence for further experiments.

### MTT assay and combination index

MTT assay was conducted to assess the impact of the experimental compounds on cell viability, following the methodology outlined by Loosdrecht et al. and Shukal et al. SKOV-3 human ovarian cancer cells were plated in 96-well plates at a concentration of  $1 \times 10^4$  cells/well. The cells were maintained for 36 h in DMEM-F12 media with 10% FBS in a CO<sub>2</sub> (5%) incubator at 37 °C. After 36 h, the cells were exposed to varying concentrations of RGZ (0.1  $\mu$ M, 1  $\mu$ M, 10  $\mu$ M, 2  $\mu$ M, 50  $\mu$ M, 75  $\mu$ M) and PTX (1 nM, 5 nM, 10 nM, 25 nM, 50 nM and 100 nM). In a combination study, five different concentrations of RGZ (0.1  $\mu$ M, 0.25  $\mu$ M, 0.5  $\mu$ M, 1  $\mu$ M, 2.5  $\mu$ M and 5  $\mu$ M) were combined each with 1 nM of PTX to determine the IC<sub>50</sub> value. Following a 24-hour incubation period, 10  $\mu$ l of MTT (3-(4,5-dimethylthiazol-2-yl)-2,5-diphenyltetrazolium bromide) solution in PBS (phosphate buffer saline) (5 mg/ml) was added to each well and incubated for an additional 4 hours at 37 °C. The media was then removed, and formazan crystals that had formed were dissolved in 100  $\mu$ l of DMSO. Absorbance levels



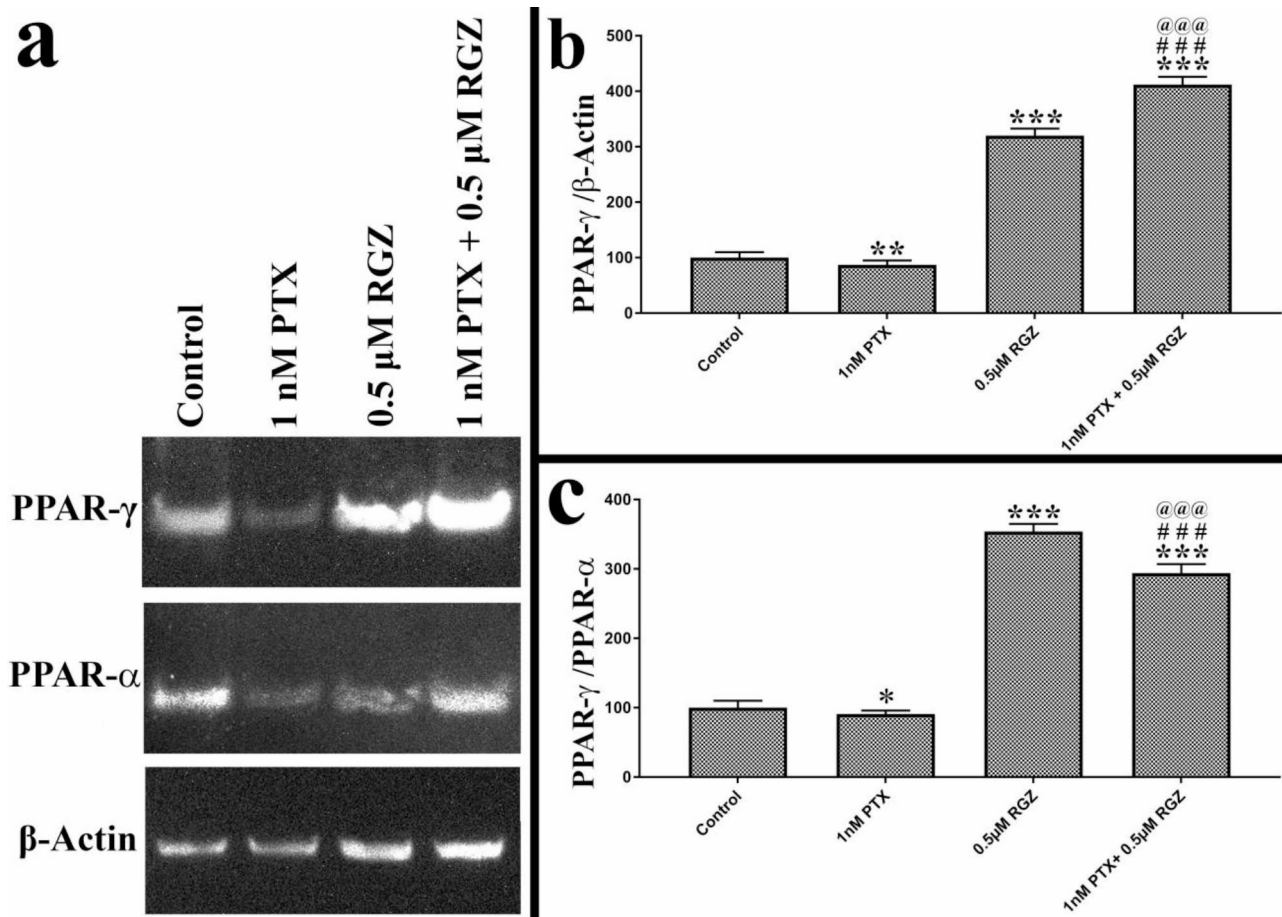


**Fig. 7.** Effect of paclitaxel (PTX) and rosiglitazone (RGZ) on the expression of PPAR-γ protein expression in SKOV-3 ovarian cancer cells. β-actin and PPAR-α were used as housekeeping genes. Error bars represent the mean ± SEM of three independent experiments. \*\*\* < 0.001 as compared to that of the control. ### < 0.001 as compared to that of the PTX alone. @@@ < 0.001 as compared to that of the RGZ alone.

were measured at 570 nm using a microplate reader (Bio-Tek Epoch microplate spectrophotometer, Vermont, USA). Compusyn software was used to find out the combination index value for the synergistic treatment of RGZ and PTX.

#### RNA extraction

RNA was isolated from both treated and untreated cells following the protocol outlined by Heidary and colleagues in 2014. A minimum of  $10^6$  cells were used to extract RNA. Treated cells (1 nM PTX + 0.5 μM RGZ) in were first washed by PBS. After aspiration of PBS as much as possible, TRIzol was added. After incubation for 5 min at room temperature, centrifugation was done at 10,000 rpm for 5 min. Carefully the aqueous phase was removed using a pipette and placed in another 1.5 ml Eppendorf tube. Isopropanol was added to the aqueous phase and mixed gently. Centrifugation was done at 14,000 rpm for 20 min followed by incubation for 5 min at room temperature. Poured off the isopropanol and added 1 ml 75% ethanol in DEPC-treated H<sub>2</sub>O. Mix it gently and centrifuged at 10,000 rpm for 5 min. After pouring off ethanol, a barely visible pellet was found of RNA. The extracted RNA was then dissolved in 30 μL of nuclease-free water. The quantity and quality of the RNA were measured using the Agilent 2100 Bioanalyzer from Agilent Technologies (USA) and the Qubit 4 Fluorometer from Thermo Fisher Scientific (USA).

#### Quantitative gene expression using real-time PCR

The RNA extracted from cells was converted into complementary DNA (cDNA) using the iScript cDNA Synthesis Kit from Bio-Rad Laboratories (USA), following the provided instructions. The cDNA was then amplified through real-time PCR on the AriaMx Real-time PCR System by Agilent Technologies (USA), using specific primer sequences according to the manufacturer's protocol. The upstream and downstream primer sequences of stemness marker genes are as follows: OCT4 (F): CTTGAATCCC GAATGGAAGGG, OCT4 (R): CCTTCCCAAATAGAACCCCA, NANOG (F): AAGGTCCTCCGGTCAAGAAACAG, NANOG (R): CTTCTGCGTCACACCATTGC, EHF (F): CCTTTGGTCTTCCCATCACA, EHF (R): GCCTCTATTTTCTCACTCCA. The mRNA expression levels of the target genes were compared to a control group using the  $2^{-\Delta\Delta CT}$  method.

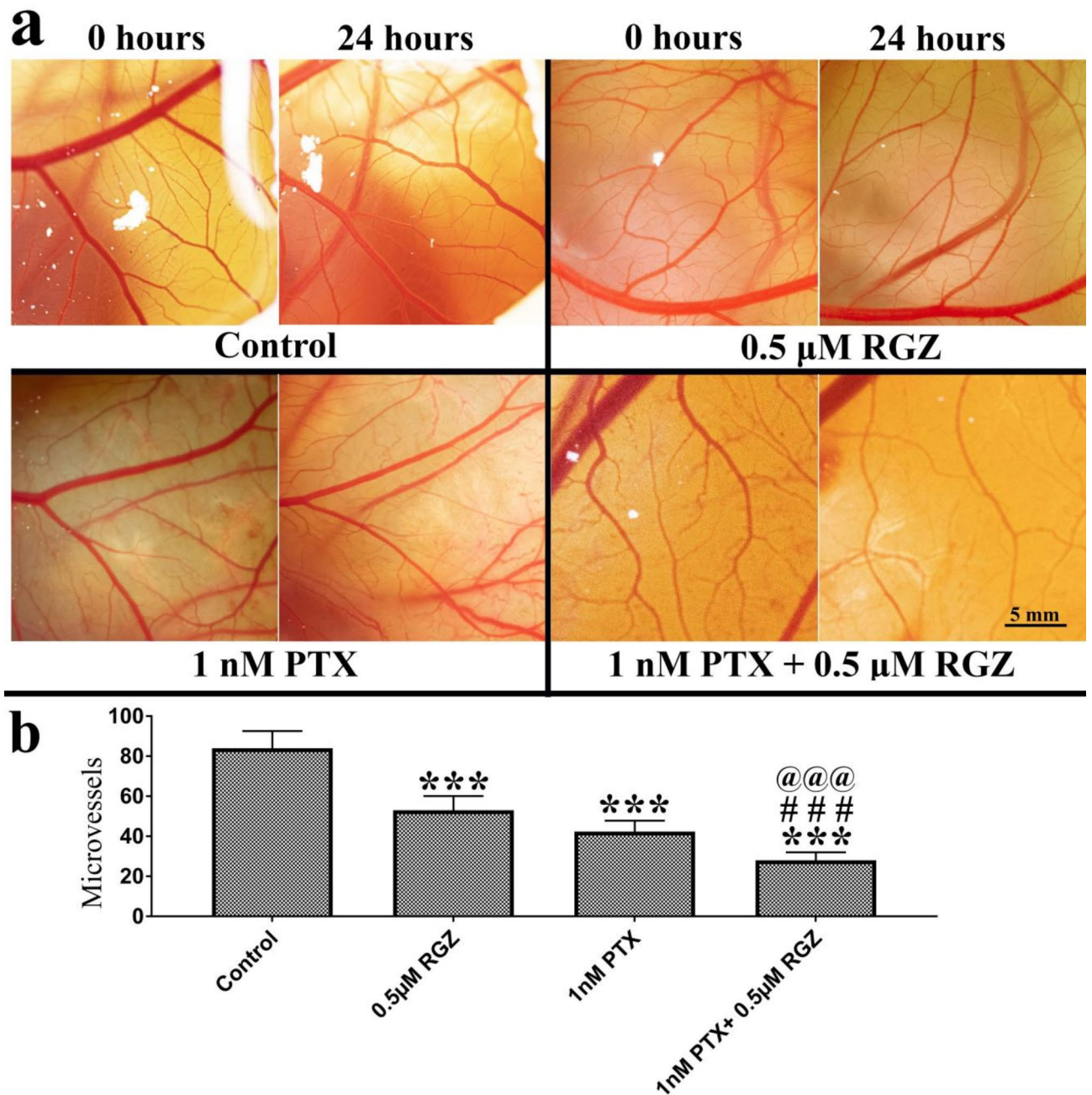


**Fig. 8.** Effect of paclitaxel (PTX) and rosiglitazone (RGZ) on the angiogenesis in chicken eggs. **(a)** Blood vessels in 7-day-old chicken eggs treated with PTX, RGZ, and their combination. Bar 5 mm. **(b)** Alteration in several micro-vessels. Error bars represent the mean  $\pm$  SEM of three independent experiments. \*\*\* < 0.001 as compared to that of the control. \*\*\* < 0.001 as compared to that of the PTX alone. @@@ < 0.001 as compared to that of the RGZ alone.

#### Cell cycle analysis

Cells were planted in a 6-well at a concentration of  $0.5 \times 10^6$  cells per well. After 24 h of being treated with drugs RGZ and PTX, the cells were fixed in 1 ml of 70% ethanol. To analyze them using flow cytometry, 1 ml of a 50  $\mu$ g/ml solution of propidium iodide (PI) in PBS from Invitrogen kit was added to the preserved cells. Subsequently, the samples were incubated for 30 min at 4°C before being examined using a Cytoflex LS (Beckman Coulter flow cytometry) as per the guidelines provided by the cell cycle kit BD™ DNA QC Particles, BD Biosciences (USA).

#### Apoptosis assay

Following the treatment of PTX and RGZ (1 nM + 0.5  $\mu$ M), the proportion of cells undergoing programmed cell death was quantified by utilizing the Annexin V- fluorescein isothiocyanate (FITC)/PI from kit BD Pharmingen™.

FITC Annexin V Apoptosis Detection Kit with the Cytoflex LS (Beckman Coulter flow cytometry) as per the guidelines provided by the manufacturer Beckman Coulter Life Sciences (USA).

### Nuclear fragmentation

Following a 24-hour treatment period, the SKOV-3 cell monolayers were subjected to staining with 10 µg/ml of propidium iodide (PI) from BD Biosciences (USA) in PBS for 5 min. The stained cells were then observed using the ZOE™ Fluorescent Cell Imager (USA). Subsequently, the fragmented and total numbers of nuclei were quantified in 10 specific fields from each sample.

### Evaluation of mitochondrial membrane potential (MMP)

Following the treatment, the cells underwent staining with JC-1 (1 mg/ml) and were then placed in an incubator at 37°C for 15 min in a dark environment. The stained samples were observed using a fluorescent microscope (Axioskope II, Carl Zeiss, Oberkochen, Germany). The intensity of the staining captured in the images through the red and green channels was quantified using Image J software.

### Western blotting

To conduct western blotting, cells were grown in six-well plates. Following treatment, the cells were washed with cold PBS and then collected in a 1X sample buffer. After a brief sonication, the cell lysate was centrifuged at 12,000g for 10 min at 4 °C, and the resulting supernatant was transferred to a new tube. The total protein content was determined using the BCA protein assay kit. Equal amounts of protein were loaded onto Bis-Tris gradient gels (ThermoFisher) in each well. The gels were then subjected to electrophoresis at 100 V until the marker proteins (BioRad Laboratories, USA) were separated. Subsequently, the proteins were transferred onto a nitrocellulose membrane. The membrane was blocked with 5% BSA and then incubated with a primary antibody overnight at 4 °C. Following this, the membrane was exposed to an anti-rabbit or anti-mouse antibody tagged with horseradish peroxidase (HRP) for an hour at 37 °C. The membrane was then washed with tris-buffered saline containing 0.1% Tween 20 detergent (TBST), and the protein bands were visualized using chemiluminescence ECL substrate (BioRad Laboratories, USA). The images were captured using a gel doc system, and the intensities of the bands were quantified using ImageJ software (version 1.45, NIH, Bethesda, Maryland, USA).

### In vivo chick chorioallantois membrane (CAM) angiogenesis assay

Obtained from a government poultry farm in Makarba, Ahmadabad, Gujarat, India, fertilized Rhode Island Red hen eggs that had been incubated for six days were used in the study. The eggs were kept in an incubator set at a temperature of  $37 \pm 1$  °C with 60% humidity for 24 h. The CAM assay, as outlined by Lokman et al.<sup>31</sup> and Rathaur et al.<sup>32</sup>, was carried out. To conduct the assay, a small opening was delicately made at the broader end of each egg on the eighth day. Various concentrations of RGZ and PTX in combination were then directly applied onto the CAM. The openings were sealed with sterile parafilm, and the eggs were placed back in the incubator for another 24 h. Before and after the drug treatment, images of the blood vessels were captured using a mirror lens camera from Sony, Japan, paired with a 90 mm macro lens from Sony, Japan. The level of angiogenesis was determined by counting the number of micro-vessels at 24- and 0 h post-treatment.

### Statistical analysis

The results were expressed as mean  $\pm$  SEM. Statistical analyses were conducted using GraphPad Prism version 7.0. A one-way analysis of variance (ANOVA) followed by Tukey's test was utilized to compare the means of multiple groups. A p-value of  $\leq 0.05$  was considered statistically significant.

### Data availability

The datasets used and/or analysed during the current study available from the corresponding author on reasonable request.

Received: 13 May 2024; Accepted: 24 September 2024

Published online: 28 December 2024

### References

1. Bray, F. et al. Global cancer statistics 2022: GLOBOCAN estimates of incidence and mortality worldwide for 36 cancers in 185 countries. *Cancer J. Clin.* **74** (3), 229–263 (2024).
2. Xiao, Y., Bi, M., Guo, H. & Li, M. Multi-omics approaches for biomarker discovery in early ovarian cancer diagnosis. *EBioMedicine* **79**, 1 (2022).
3. Sambasivan, S. Epithelial ovarian cancer. *Cancer Treat. Res. Commun.* **33**, 100629 (2022).
4. Roett, M. A. & Evans, P. Ovarian cancer: an overview. *Am. Family Phys.* **80** (6), 609–616 (2009).
5. Mhatre, A. et al. Multi-omics analysis of the Indian ovarian cancer cohort revealed histotype-specific mutation and gene expression patterns. *Front. Genet.* **6**, 1102114 (2023).
6. Yang, C. et al. Immunotherapy for ovarian cancer: adjuvant, combination, and neoadjuvant. *Front. Immunol.* **11**, 577869 (2020).
7. Agarwal, R. & Kaye, S. B. Ovarian cancer: strategies for overcoming resistance to chemotherapy. *Nat. Rev. Cancer.* **3** (7), 502–516 (2003).
8. Carr, C., Ng, J. & Wigmore, T. The side effects of chemotherapeutic agents. *Curr. Anaesth. Crit. Care.* **19** (2), 70–79 (2008).
9. Feng, L. X., Li, M., Liu, Y. J., Yang, S. M. & Zhang, N. Synergistic enhancement of cancer therapy using a combination of ceramide and docetaxel. *Int. J. Mol. Sci.* **15** (3), 4201–4220 (2014).
10. Duarte, D. & Vale, N. Evaluation of synergism in drug combinations and reference models for future orientations in oncology. *Curr. Res. Pharmacol. Drug Discov.* **3**, 100110 (2022).
11. Rodrigues, R., Duarte, D. & Vale, N. Drug repurposing in cancer therapy: influence of patient's genetic background in breast cancer treatment. *Int. J. Mol. Sci.* **23** (8), 4280 (2022).

12. Jean-Pierre, J. Drug repositioning: a brief overview. *J. Pharm. Pharmacol.* **72**, 1 (2020).
13. Hovington, J. P., Al-Lazikani, B. & Hopkins, A. L. How many drug targets are there?. *Nat. Rev. Drug Discov.* **5**(12), 993–996 (2006).
14. Houseknecht, K. L., Cole, B. M. & Steele, P. J. Peroxisome proliferator-activated receptor gamma (PPAR $\gamma$ ) and its ligands: a review. *Domest. Anim. Endocrinol.* **22** (1), 1–23 (2002).
15. Al-Alem, L., Southard, R. C., Kilgore, M. W. & Curry, T. E. Specific thiazolidinediones inhibit ovarian cancer cell line proliferation and cause cell cycle arrest in a PPAR $\gamma$  independent manner. *PLoS One.* **6** (1), e16179 (2011).
16. Lin, C. F. et al. Rosiglitazone regulates anti-inflammation and growth inhibition via PTEN. *BioMed Res. Int.* (2014).
17. Zhang, W. et al. PPAR $\gamma$  activator rosiglitazone inhibits cell migration via upregulation of PTEN in human hepatocarcinoma cell line BEL-7404. *Cancer Biol. Ther.* **5** (8), 1008–1014 (2006).
18. Dang, Y. F., Jiang, X. N., Gong, F. L. & Guo, X. L. New insights into molecular mechanisms of rosiglitazone in monotherapy or combination therapy against cancers. *Chemico-Biol. Interact.* **296**, 162–170 (2018).
19. Kim, S. Y. et al. PPAR $\gamma$  induces growth inhibition and apoptosis through upregulation of insulin-like growth factor-binding protein-3 in gastric cancer cells. *Braz. J. Med. Biol. Res.* **48**, 226–233 (2015).
20. Mody, M. et al. Rosiglitazone sensitizes MDA-MB-231 breast cancer cells to anti-tumour effects of tumour necrosis factor- $\alpha$ , CH11 and CYC202. *Endocrine-Relat. Cancer.* **14**(2), 305–315 (2007).
21. Bonofiglio, D. et al. Combined low doses of PPAR $\gamma$  and RXR ligands trigger an intrinsic apoptotic pathway in human breast cancer cells. *Am. J. Pathol.* **175** (3), 1270–1280 (2009).
22. Wang, Z. et al. The PPAR $\gamma$  agonist rosiglitazone enhances the radio sensitivity of human pancreatic cancer cells. *Drug Des. Dev. Ther.* 3099–3110 (2020).
23. Lehmann, J. M. et al. An antidiabetic thiazolidinedione is a high affinity ligand for peroxisome proliferator-activated receptor  $\gamma$  (PPAR $\gamma$ ). *J. Biol. Chem.* **270** (22), 12953–12956 (1995).
24. Panigraphy, D., Huang, S., Kieran, M. W. & Kaipainen, A. PPAR $\gamma$  as a therapeutic target for tumor angiogenesis and metastasis. *Cancer Biol. Ther.* **4**(7), 687–693 (2005).
25. Ren, Q. C., Peng, Z. L. & Tan, X. Proliferation and apoptosis effect of rosiglitazone on human ovarian cancer cell line SKOV3. *Sichuan da xue xue bao. Yi xue ban Journal of Sichuan University. Med. Sci. Ed.* **40** (2), 217–222 (2009).
26. Sara Vignati, V., Albertini, G. M., Carbone, C. V. & Catapano Induction of cell cycle arrest and apoptosis by ligands of peroxisome proliferator-activated receptor gamma in human ovarian cancer cells. *Cancer Res.* **64**(7) (2004).
27. Zhang, H. et al. Suppression of multidrug resistance by rosiglitazone treatment in human ovarian cancer cells through downregulation of FZD1 and MDR1 genes. *Anti-Cancer Drugs* **26**(7), 706–715 (2015).
28. Van de Loosdrecht, A. A., Beelen, R. H., Ossenkuppe, G., Broekhoven, M. G. & Langenhuijsen, M. M. A tetrazolium-based colorimetric MTT assay to quantitate human monocyte mediated cytotoxicity against leukemic cells from cell lines and patients with acute myeloid leukemia. *J. Immunol. Methods.* **174** (1–2), 311–320 (1994).
29. Shukal, D. et al. Dichloroacetate prevents TGF $\beta$ -induced epithelial-mesenchymal transition of retinal pigment epithelial cells. *Exp. Eye Res.* **197**, 108072 (2020).
30. Pahlevan Kakhki, M. TRIzol-based RNA extraction: a reliable method for gene expression studies. *J. Sci. Islamic Republic Iran* **25**(1), 13–17 (2014).
31. Lokman, N. A., Elder, A. S., Ricciardelli, C. & Oehler, M. K. Chick chorioallantoic membrane (CAM) assay as an in vivo model to study the effect of newly identified molecules on ovarian cancer invasion and metastasis. *Int. J. Mol. Sci.* **13** (8), 9959–9970 (2012).
32. Rathaur, P. et al. Network pharmacology-based evaluation of natural compounds with paclitaxel for the treatment of metastatic breast cancer. *Toxicol. Appl. Pharmacol.* **423**, 115576 (2021).
33. Lehár, J. et al. Synergistic drug combinations tend to improve therapeutically relevant selectivity. *Nat. Biotechnol.* **27**(7), 659–666 (2009).
34. Miao, R. et al. Rosiglitazone and retinoic acid inhibit proliferation and induce apoptosis in the HCT-15 human colorectal cancer cell line. *Exp. Ther. Med.* **2**(3), 413–417 (2011).
35. Shigeto, T., Yokoyama, Y., Xin, B. & Mizunuma, H. Peroxisome proliferator-activated receptor  $\alpha$  and  $\gamma$  ligands inhibit the growth of human ovarian cancer. *Oncol. Rep.* **18** (4), 833–840 (2007).
36. Sheu, W. H., Ou, H. C., Chou, F. P., Lin, T. M. & Yang, C. H. Rosiglitazone inhibits endothelial proliferation and angiogenesis. *Life Sci.* **78**(13), 1520–1528 (2006).
37. Wang, H. Y. et al. Rosiglitazone elevates sensitization of drug-resistant oral epidermoid carcinoma cells to vincristine by G2/M-phase arrest, independent of PPAR- $\gamma$  pathway. *Biomed. Pharmacother.* **83**, 349–361 (2016).
38. Ramos-Nino, M. E. & Littenberg, B. A novel combination: ranpirnase and rosiglitazone induce a synergistic apoptotic effect by down-regulating Fra-1 and Survivin in cancer cells. *Mol. Cancer Ther.* **7** (7), 1871–1879 (2008).
39. Nguyen, C. & Pandey, S. Exploiting mitochondrial vulnerabilities to trigger apoptosis selectively in cancer cells. *Cancers.* **11** (7), 916 (2019).
40. Yang, Y. et al. The mechanisms of action of mitochondrial targeting agents in cancer: inhibiting oxidative phosphorylation and inducing apoptosis. *Front. Pharmacol.* **2023 Oct.** **25**, 1243613 (2023).
41. Cao, L. Q. et al. Upregulation of PTEN involved in rosiglitazone-induced apoptosis in human hepatocellular carcinoma cells 1. *Acta Pharmacol. Sin.* **28**(6), 879–887 (2007).
42. Wang, Z., Gao, J., Ohno, Y., Liu, H. & Xu, C. Rosiglitazone ameliorates senescence and promotes apoptosis in ovarian cancer induced by olaparib. *Cancer Chemother. Pharmacol.* **85**, 273–284 (2020).
43. Liu, J. J., Zhang, Y., Xiao, R. Z. & Lin, D. J. Peroxisome proliferator-activated receptor  $\gamma$  (PPAR- $\gamma$ ) agonist rosiglitazone (RGZ) inhibits HL-60 cell growth by induction of apoptosis. *Lab. Med.* **40** (5), 297–302 (2009).
44. Wang, G., Zhou, H., Gu, Z., Gao, Q. & Shen, G. Oct4 promotes cancer cell proliferation and migration and leads to poor prognosis associated with the survivin/STAT3 pathway in hepatocellular carcinoma. *Oncol. Rep.* **40** (2), 979–987 (2018).
45. Mohiuddin, I. S., Wei, S. J. & Kang, M. H. Role of OCT4 in cancer stem-like cells and chemotherapy resistance. *Biochim. Biophys. Acta (BBA) Mol. Basis Dis.* **1866**(4), 165432 (2020).
46. Wang, Y. D. et al. OCT4 promotes tumorigenesis and inhibits apoptosis of cervical cancer cells by miR-125b/BAK1 pathway. *Cell Death Dis.* **4** (8), e760 (2013).
47. Jeter, C. R., Yang, T., Wang, J., Chao, H. P. & Tang, D. G. Concise review: NANOG in cancer stem cells and tumor development: an update and outstanding questions. *Stem Cells.* **33** (8), 2381–2390 (2015).
48. Gao, L. et al. EHF enhances malignancy by modulating AKT and MAPK/ERK signaling in non-small cell lung cancer cells. *Oncol. Rep.* **45** (6), 1–2 (2021).
49. Cheng, Z. et al. Knockdown of EHF inhibited the proliferation, invasion and tumorigenesis of ovarian cancer cells. *Mol. Carcinog.* **155** (6), 1048–1059 (2016).
50. Aljada, A., O'Connor, L., Fu, Y. Y. & Mousa, S. A. PPAR $\gamma$  ligands, rosiglitazone and pioglitazone, inhibit bFGF-and VEGF-mediated angiogenesis. *Angiogenesis.* **11**, 361–367 (2008).
51. Bocci, G., Di Paolo, A. & Danesi, R. The pharmacological bases of the antiangiogenic activity of paclitaxel. *Angiogenesis.* **16**, 481–492 (2013).
52. Alatise, K. L., Gardner, S. & Alexander-Bryant, A. Mechanisms of drug resistance in ovarian cancer and associated gene targets. *Cancers.* **14** (24), 6246 (2022).

## Acknowledgements

We greatly appreciate and acknowledge DBT-SAHAJ imaging and flow cytometry national facility, Department of Biotechnology, Government of India located at Ahmedabad University for providing access to the Flow Cytometer.

## Author contributions

Conceptualization: K.J., A.V. and V.T.; Methodology: B.P., A.P., F.M.; Visualization and DATA analyzing: K.J., S.P., B.P. and A.P.; Supervision: K.J., A.V. and V.T.; Writing—original draft: B.P. and K.J. ; Writing—review and editing: B.P., K.J., S.P. and A.P. All authors have read and agreed to the published version of the manuscript.

## Declarations

### Competing interests

The authors declare no competing interests.

## Additional information

**Supplementary Information** The online version contains supplementary material available at <https://doi.org/10.1038/s41598-024-74277-9>.

**Correspondence** and requests for materials should be addressed to K.J.S.

**Reprints and permissions information** is available at [www.nature.com/reprints](http://www.nature.com/reprints).

**Publisher's note** Springer Nature remains neutral with regard to jurisdictional claims in published maps and institutional affiliations.

**Open Access** This article is licensed under a Creative Commons Attribution-NonCommercial-NoDerivatives 4.0 International License, which permits any non-commercial use, sharing, distribution and reproduction in any medium or format, as long as you give appropriate credit to the original author(s) and the source, provide a link to the Creative Commons licence, and indicate if you modified the licensed material. You do not have permission under this licence to share adapted material derived from this article or parts of it. The images or other third party material in this article are included in the article's Creative Commons licence, unless indicated otherwise in a credit line to the material. If material is not included in the article's Creative Commons licence and your intended use is not permitted by statutory regulation or exceeds the permitted use, you will need to obtain permission directly from the copyright holder. To view a copy of this licence, visit <http://creativecommons.org/licenses/by-nc-nd/4.0/>.

© The Author(s) 2024